Science & Technology Development Journal 2022, 25(4):2548-2556

Open Access Full Text Article

Research article

Nanosers devices based on Au-studded ZnO nanorod for R6G detection

Nguyen Duy Khanh*, Luong Minh Thu, Pham Dien Khoa, Le Van Ngoc, Vu Thi Hanh Thu*, Le Vu Tuan Hung*

ABSTRACT

Introduction: The prospect of wielding semiconductor–noble metal hybrid nanomaterials as surface-enhanced Raman scattering (SERS) substrates for the ultrasensitive detection of organic molecules in sensing applications has attracted ever-increasing attention. In this study, nanoSERS devices based on Au-studded ZnO nanorods (Au/ZnO) were fabricated using a facile photochemical deposition method for the detection of low-concentration rhodamine 6G (R6G) molecules. **Methods:** Analytical techniques such as SEM, EDX, XRD, and UV–Vis spectroscopy were utilized to investigate the morphology, elemental composition, crystalline structure, and optical absorption of the Au/ZnO nanostructure, respectively. Raman scattering spectroscopy was used to evaluate rhodamine 6G. **Results:** The results show that vertically well-aligned ZnO nanorods (NRs) were effectively grown on the seeded glass substrate at 90°C for 4 h, and Au nanoparticles (NPs) with a diameter of approximately 20 nm were successfully deposited onto their surface. Comparing the obtained Au/ZnO substrate to the ZnO NRs and glass substrates, it exhibited superior SERS performance with R6G at a low concentration of 10^{-3} M. Significantly, it was found that the Au/ZnO for the R6G sensitive limit was approximately 10^{-9} M. This could be explained due to the surface plasmon resonance (SPR)-induced electromagnetic field enhancement of Au NPs as well as the charge-transfer mechanism between the Au/ZnO substrate and adsorbed R6G molecules under 532 nm laser excitation. **Conclusion:** This work demonstrates the potential SERS activity of Au/ZnO substrates, which can identify organic substances at trace levels using the Raman analysis method.

Key words: Au nanoparticles, Rhodamine 6G, SERS, ZnO nanorods

Faculty of Physics and Engineering Physics, VNUHCM-University of Science, Viet Nam

Correspondence

Nguyen Duy Khanh, Faculty of Physics and Engineering Physics, VNUHCM-University of Science, Viet Nam

Email: ndkhanh@hcmus.edu.vn

Correspondence

Vu Thi Hanh Thu, Faculty of Physics and Engineering Physics, VNUHCM-University of Science, Viet Nam

Email: vththu@hcmus.edu.vn

Correspondence

Le Vu Tuan Hung, Faculty of Physics and Engineering Physics, VNUHCM-University of Science, Viet Nam

Email: lvthung@hcmus.edu.vn

History

- Received: 2022-07-07
- Accepted: 2023-01-13
- Published: 2023-01-20

DOI : 10.32508/stdj.v25i4.3966

INTRODUCTION

In recent years, surface-enhanced Raman scattering (SERS) has attracted scientific interest due to its wide applications in many fields, including pesticide detection in foody[1,2], chemical and biological sensing[3], and the diagnosis of cancer cells[4,5]. SERS is a technique that allows the detection of extremely low amounts of analyte molecules adsorbed on a typical nanostructured metal surface. To achieve high detection sensitivity, nanoSERS devices should possess not only a high density of interparticle nanoscale gaps (known as "hot spots") to significantly enhance the local electromagnetic fields upon laser excitation but also a large surface area to adsorb plenty of analyte molecules[6,7].

The three-dimensional (3D) nanostructured substrates offer significant advantages when used as SERS substrates over 1D and 2D equivalents. They can significantly increase the overall surface area to load plasmonic metal nanoparticles for more "hot spots" and ease the adsorption of more target analytes as a given steric platform with considerable extension along the z-axis dimension[8]. One of the promising strategies for their development is the combination of noble metal plasmonic nanostructures and semiconductor oxides. Previous publications demonstrated that most SERS substrates based on noble gold or silver nanostructures, such as nanoparticles, nanorods, nanowires, and thin films, possess Raman signal enhancement factors on the order of 10^2 to 10^9, which is due to enhancement in the local electromagnetic field (excited by localized surface plasmon resonance of noble metals)[9–12]. In addition, other studies showed that using semiconductors such as ZnO[13], TiO_2[14], and SnO_2[15] could also generate a weak SERS activity with an enhancement factor on the order of 10^3 due to chemical enhancement supported by the semiconductor (caused by charge-transfer interactions)[16,17]. Therefore, when these semiconductors are combined with noble metals, noble metal/semiconductor substrates can significantly improve SERS activity due to the contribution of both electromagnetic enhancement and chemical enhancement.

Among those semiconductors, ZnO is widely used in the visible and near-UV wavelength regions because it is an n-type semiconductor with a direct

Cite this article : Khanh N D, Thu L M, Khoa P D, Ngoc L V, Thu V T H, Hung L V T. **Nanosers devices based on Au-studded ZnO nanorod for R6G detection**. *Sci. Tech. Dev. J.;* 2022, 25(4):2548-2556.

wide band of 3.37 eV and a large excitation binding energy of 60 meV. In particular, ZnO nanorods (NRs) are promising nanostructures for the fabrication of SERS substrates because of their high surface-to-volume-ratio morphology and ease of preparation [16,18–20]. This system, with a high surface area, could attach plasmonic metal nanoparticles onto different dimensions of the side surfaces and top ends of the ZnO NRs, forming a high density of "hot spots" and directly trapping target analytes onto the "hot spots" to achieve high-performance 3D SERS substrates. For instance, the Au/ZnONRs/G SERS sensor was revealed to exhibit very high sensitivity in SERS signals toward rhodamine 6G molecules at a concentration of 10^{-9} M and an enhancement factor of $2.3x10^6$ [19]. Arrays of ZnO NRs decorated with Au nanoparticles manifested high SERS sensitivity to melamine and a detection limit as low as 10^{-10} M [20]. In addition, ZnO NRs/Ag possessed an enhancement factor of $1.98x10^7$ and a detection limit as low as 10^{-12} M for testing rhodamine 6G molecules [21]. ZnO NR/noble-metal hybrid substrates were assured, by means of these results, for their fascinating SERS properties. Ag nanoparticles (NPs) have been demonstrated to be extremely effective in enhancing Raman scattering, but they are susceptible to oxidation in air [22]. Therefore, Ag NP-based SERS substrates are limited in some applications, especially the reusability of these substrates. This is a serious drawback not only in terms of economy but also in terms of reproducibility. Instead, Au NPs with excellent oxidation resistance along with low fluorescence were selected to assemble onto the surface of ZnO NRs. Although there are many approaches to attaching metal nanoparticles onto ZnO NRs, expensive-sophisticated apparatuses, high manufacturing costs, and difficulty in controlling the growth process remain challenges for fabricating effective SERS substrates. To tackle this problem, the photochemical synthesis method was employed. Based on the facile photochemical reduction process of Au ions and the overgrowth of Au NPs on the surface of ZnO NRs, Au nanoparticle-decorated ZnO nanorods were successfully constructed as SERS-active substrates.

For the above reasons, in this study, a simple, economic and practical process was applied to fabricate ZnO NRs decorated with Au NPs, following the wet chemical pathway and photochemical deposition. It is well known that the controlled growth of ZnO NRs with the solution-phase method is cost-effective and scalable to large areas, making the fabrication process very appealing for many practical applications. Then, the photochemical deposition method was used to deposit Au NPs on the surface of ZnO NRs (Au/ZnO), resulting in the successful formation of 3D hybrid SERS substrates. By using rhodamine 6G (R6G) as a probe molecule, the SERS activity of the fabricated Au/ZnO substrate was demonstrated to be highly sensitive with a low detection limit of 10^{-9} M. Furthermore, based on the photocatalytic properties of the Au/ZnO hybrid substrate, R6G molecules could be almost completely removed from the substrate through UV irradiation to provide a reusable SERS substrate. With its interesting advantages in sensitivity and reusability, Au/ZnO nanoSERS has promising potential for chemical, physical, and biological sensing applications, especially for testing trace levels of organic contaminants.

EXPERIMENT

Materials

Zinc acetate dihydrate ($Zn(CH_3COO)_2.2H_2O$, $\geq$ 98%), ethanolamine (MEA, C_2H_7NO, $\geq$ 99.0%), ethylene glycol monomethyl ether ($C_3H_8O_2$, $\geq$ 99.8%), zinc nitrate hexahydrate ($Zn(NO_3)_2.6H_2O$, 98%), hexamethylenetetramine (HMTA, 99%), gold(III) chloride trihydrate ($HAuCl_4.3H_2O$, $\geq$ 99.9%), rhodamine 6G dye (R6G, $C_{28}H_{31}N_2O_3Cl$, 99%), sodium hydroxide (NaOH) and methanol (CH_3OH). All chemicals were purchased from Sigma–Aldrich and used without further purification. Double distilled water was used throughout the experiments.

Preparation of ZnO nanorods

The ZnO NRs on the glass substrates were fabricated following a two-step process. First, zinc acetate dihydrate was dissolved in a mixture of ethylene glycol monomethyl ether and ethanolamine at room temperature to form a solution. The solution was stirred at 60°C for 30 min to yield a clear and homogeneous sol solution. The cleaned glass substrate was dipped into the above sol solution for 10 min, withdrawn at a rate of 2 cm/min by the dip-coating method, and then annealed at 250° C for 30 min for solvent evaporation to form a seed layer. In the next step, the ZnO NRs were grown on the ZnO seed layer by a wet chemical process, which began by mixing zinc nitrate hexahydrate 0.1 M and hexamethylenetetramine 0.1 M in 200 ml of distilled water. The ZnO seed-layer-coated glass substrates were immersed in the prepared aqueous solution and heated at a temperature of 90° C with a growth time of 4 h. After this process, the samples were rinsed with distilled water several times and naturally dried in air. Finally, ZnO NRs on glass substrates were obtained.

Fabrication of Au nanoparticle-decorated ZnO nanorods

To deposit Au NPs on the ZnO NRs, the ZnO NRs were immersed in a mixed solution containing 20 ml $HAuCl_4.3H_2O$ 1 mM aqueous solution and 2 ml methanol and irradiated continuously with a UV lamp for 30 min at a distance of 30 cm from the source to the samples. The pH of the solution was controlled by adding 1 M sodium hydroxide until the pH was equal to 8. Under the illumination of UV light, electron-hole pairs were generated and transferred to the surface of the ZnO NRs. Au^{3+} ions were reduced to Au^0 at the surface of ZnO NRs, resulting in the formation of Au -decorated ZnO NR heterostructures (the samples obtained were denoted as Au/ZnO). The reduction process can be represented by the following equations:

$$ZnO \rightarrow ZnO\,(e+h) \quad (1)$$

$$ZnO\,(e+h) \rightarrow e^- + h^+ \quad (2)$$

$$Au^{3+} + 3e^- \rightarrow Au \quad (3)$$

Finally, the samples were removed from the solution, rinsed with distilled water to eliminate residual ions and contaminations, and then dried in air at room temperature for subsequent characterization.

A schematic of the fabrication process of the Au -decorated ZnO NRs is given in Figure 1.

SERS measurement

Rhodamine 6G was used as a SERS probe molecule in our experiment. Twenty microliters of R6G solution with concentrations varying from 10^{-3} M to 10^{-9} M was dropped onto the surface of the ZnO and Au/ZnO substrates (size 1x1 cm^2) and then dried naturally in air before SERS characterization. The Raman measurements were performed at room temperature using a Horiba XploRA PLUS Raman system and were repeated five times at different positions on the same sample. The test parameters were applied as follows: a 532 nm laser was used as the exciting light, a 100x objective was used to focus the laser beam onto the sample surface and to collect the Raman signal, the size of the laser spot was approximately 1 μm, and the spectra were recorded with an accumulation time of 1. Moreover, to evaluate the reusability of the Au/ZnO SERS substrate, self-cleaning cycles of the Au/ZnO substrate were performed by immersing the substrate in distilled water and irradiating the sample under UV light for 90 min. After irradiation, the substrate was then rinsed with distilled water, dried at room temperature, and retested with Raman measurement.

Characterization

The samples were analyzed by X-ray diffraction (XRD) with Cu K radiation (Bruker D8 Advance, λ=1.5406 Å). The morphologies of the specimens were observed using scanning electron microscopy (SEM, Hitachi, S-4800). The chemical composition of the samples was examined by energy-dispersive X-ray (EDX) spectroscopy. The UV–Vis spectra were recorded with a spectrophotometer (UV–VIS Jasco V730) in absorption mode.

RESULTS

The morphology of the original ZnO NRs on the glass substrate was examined by scanning electron microscopy (SEM), as shown in Figure 2 (a and b). The typical SEM images show that the ZnO NRs are well aligned and uniform, and most of the nanorods are hexagonal in shape. The hexagonal ZnO NRs successfully grew perpendicularly on the whole surface of the glass substrate with high density. The diameter of the nanorods is in the range of 70 - 175 nm, and their length reaches approximately 1.2 μm.

After attaching Au NPs, the SEM images in Figure 2 (c and d) confirm the successful deposition of a large number of Au NPs on the surfaces of ZnO NRs prepared in a 1 mM $HAuCl_4.3H_2O$ aqueous solution. As shown in Figure 2 (a and c), a relatively high density of Au NPs with a diameter of approximately 20 nm and a random distribution formed on the top ends and side surfaces of the ZnO NRs. Additionally, compared with the original ZnO nanorods, the shapes of well-defined rods were maintained after UV irradiation. As shown in Figure 2 d, the average spacing of the neighboring nanoparticles could be estimated. The average gap between adjacent Au NPs was estimated to range from a few nanometers to several tens of nanometers. According to theoretical and experimental studies[7,19,23], there is a relationship between the internanoparticle gap and high-performance SERS activity, and metal particles show a giant electromagnetic SERS enhancement when internanoparticle gaps reach sub10 nm. Therefore, in our work, ZnO NRs decorated with Au NPs can serve as promising SERS substrates for ultrasensitive detection, as the Au/ZnO substrate possesses "hot spot" positions on the substrate surface, resulting in strong electromagnetic coupling between neighboring nanoparticles to create extremely high SERS activity.

To further verify the elemental composition of Au/ZnO, EDX spectra were obtained and are shown in Figure 3. The typical EDX analysis (Figure 3a) confirms the existence of oxygen, zinc, and gold elements,

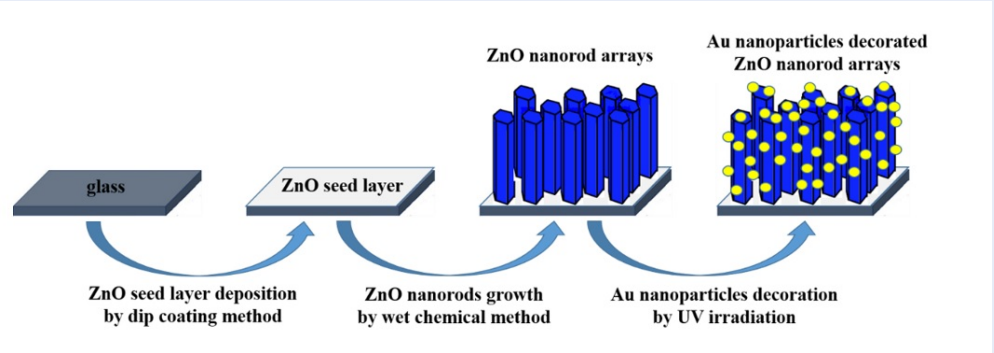

Figure 1: Schematic illustration of the preparation process of Au nanoparticle-decorated ZnO nanorod arrays for SERS substrates.

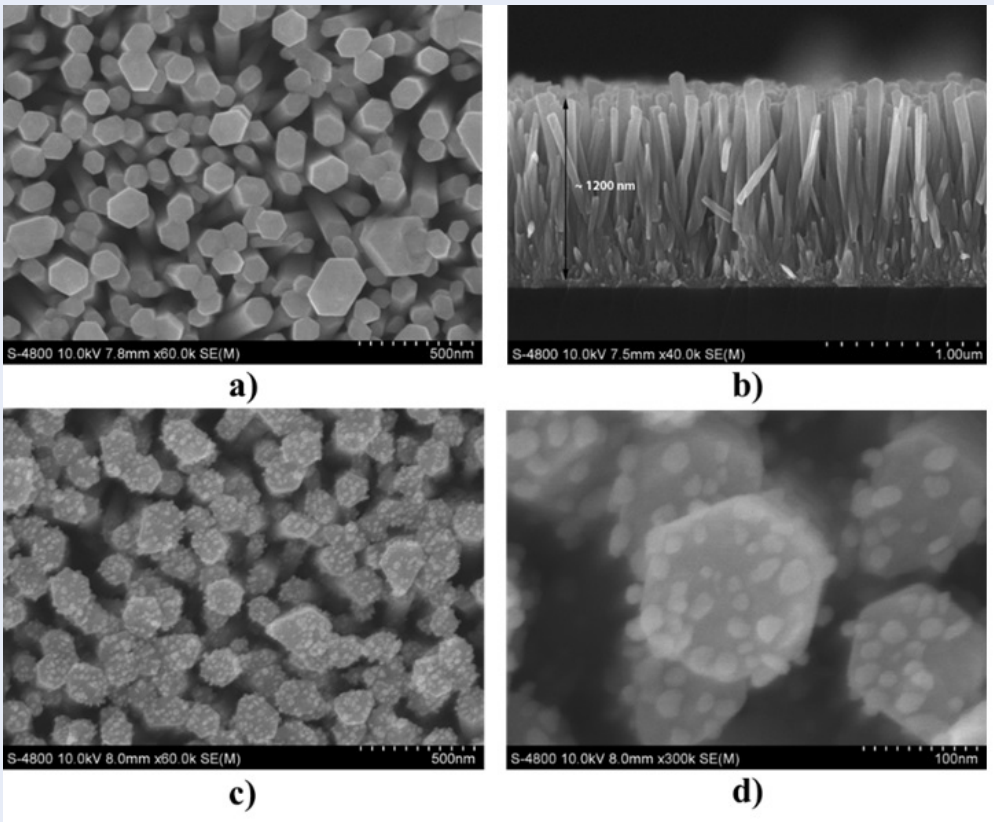

Figure 2: SEM images of ZnO NRs and Au/ZnO substrate at 1 mM $HAuCl_4.3H_2O$. (a) The surface of ZnO NRs; (b) the cross-section of ZnO NRs; (c, d) the surface of Au/ZnO.

thus assuring the successful formation of the Au NP-decorated ZnO NR heterostructure. The signals of both Zn and O are attributed to the ZnO NRs, and the signal of Au is from the Au NPs on the surface of the ZnO NRs. Moreover, the elemental mapping images in Figure 3 (b-e) illustrate that the distributions of these elements coincide with those on the whole Au/ZnO nanostructure.

The crystalline structure of ZnO NRs and Au/ZnO was investigated by X-ray diffraction. As shown in Figure 4, the ZnO NRs exhibit a highly crystalline structure. For all the samples, a peak at $2\theta = 34.4^{\circ}$ corresponding to the (002) plane of the hexagonal wurtzite ZnO structure (JCPDS card no. 36-1451) is very strong and dominant in the XRD spectra. This result reveals that the growth of ZnO NRs is perpendicular to the seeded substrates with the preferred c-axis orientation. After ZnO NRs were decorated with Au NPs, a new diffraction peak at $2\theta = 38.3^{\circ}$ (labeled with *) corresponding to the (111) plane of the fcc (face-centered cubic) Au (JCPDS card no. 04-0784) was observed, further indicating the successful decoration of Au NPs on the surface of ZnO NRs.

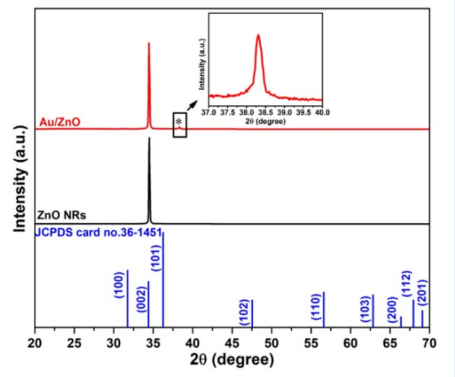

Figure 4: XRD patterns of ZnO NRs and Au/ZnO substrate at 1 mM $HAuCl_4.3H_2O$

Figure 5 shows the optical absorption spectra of the original ZnO NRs and Au/ZnO samples in the UV–Vis-NIR spectral region. For the ZnO NR sample, the presence of a typical ZnO absorption edge appears at a wavelength of approximately 380 nm, corresponding to the optical bandgap of ZnO NRs. The original ZnO NR spectrum exhibits a high absorption behavior in the UV-light region and a weak absorption in the visible and near-infrared regions. Compared to the original ZnO NRs, the absorption spectrum of Au/ZnO exhibits a characteristic surface plasmon resonance (SPR) absorption band of Au NPs located at approximately 528 nm. In addition, the absorption edge of Au/ZnO shows a slight redshift due to the interfacial coupling effect between the metal Au and semiconductor ZnO in the Au/ZnO heterostructure[24,25].

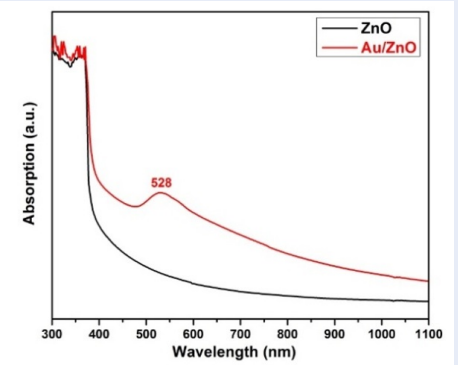

Figure 5: Optical absorption spectra of ZnO NRs and Au/ZnO substrate at 1 mM $HAuCl_4.3H_2O$

To evaluate the SERS activities of ZnO NRs and Au/ZnO, rhodamine 6G (R6G), with its well-established vibrational features, was selected as the probe molecule. Figure 6 a depicts the recorded SERS spectra of 10^{-3} M R6G adsorbed on glass, ZnO NRs, and Au/ZnO substrates. As demonstrated in Figure 6 a, there is no Raman signal with the glass substrate. When the ZnO NR substrate is used as the SERS substrate, the Raman signals of R6G molecules recorded over the substrate are weak, and some characteristic Raman signals are not observed. This result reveals that the SERS enhancement behavior between ZnO NRs and R6G molecules should be due to classical chemical enhancement. However, when the Au/ZnO substrate is used for SERS, the Raman signals of R6G are increased significantly. These Raman peaks can be attributed to the C–C–C ring in-plane bending vibration (609 cm^{-1}), C–H out-of-plane bending vibration (771 cm^{-1}), C–H in-plane bending vibration (1187 cm^{-1}), and symmetric modes of in-plane aromatic C–C stretching vibrations (1310, 1360, 1505, 1572, and 1649 cm^{-1})[26,27]. This could be explained by the SPR-induced electromagnetic field enhancement of Au NPs as well as the charge-transfer mechanism between the Au/ZnO substrate and adsorbed molecules under 532 nm laser excitation.

Subsequently, to further evaluate the SERS sensitivity of the Au/ZnO substrate, SERS spectra of R6G at various concentrations from 10^{-5} M to 10^{-9} M were also collected. As shown in Figure 6b, the SERS signal intensity of the R6G molecules gradually declines

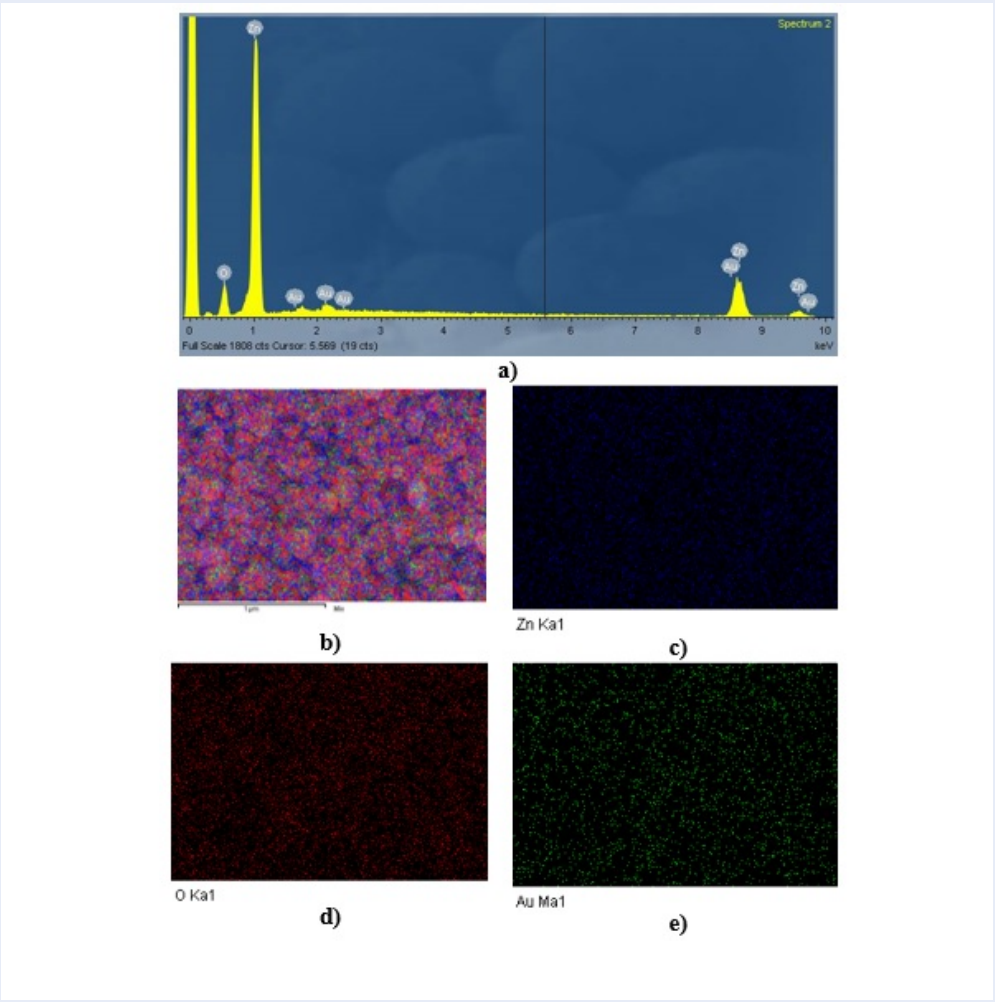

Figure 3: EDX elemental component and elemental mapping analysis of Au/ZnO substrate at 1 mM $HAuCl_4.3H_2O$. (a) EDX spectrum of Au/ZnO; (b) EDX map of the merged structure; elemental mapping images of (c) Zn, (d) O, and (e) Au.

with decreasing R6G concentration, but it can still be distinguished even if the concentration of R6G is reduced to 10^{-9} M, which indicates that the limit of detection (LOD) for R6G is determined to be approximately 10^{-9} M.

After Raman measurement, the reusability of the Au/ZnO SERS substrate was examined based on the photocatalytic activity of the Au/ZnO heterostructure. The results reveal that the R6G molecules were degraded under UV light irradiation after every self-cleaning cycle, and then the Raman signal was well reproduced, as shown in Figure 7. Under exposure to UV irradiation, electron-hole pairs are created on the surface of ZnO NRs. The electrons and holes react with oxygen and water to produce superoxide radical anions $^{\bullet}O_2^-$ and hydroxyl radicals $^{\bullet}OH$. These radicals are the main active species responsible for the decomposition of R6G into CO_2 and H_2O[28,29]. Obviously, the Au-NPs/ZnO-NRs as a SERS-active substrate showed high sensitivity and good reusability; therefore, the Au-NPs/ZnO-NR substrate is proposed as a potential SERS substrate for realistic applications.

DISCUSSION

The ZnO NR substrate was immersed in $HAuCl_4.3H_2O$ methanol/water solution and irradiated continuously with a UV lamp at a distance of 30 cm from the source to the sample to construct a high-performance 3D SERS substrate for the detection of low-concentration R6G. Under UV irradiation, the UV photon energy is absorbed

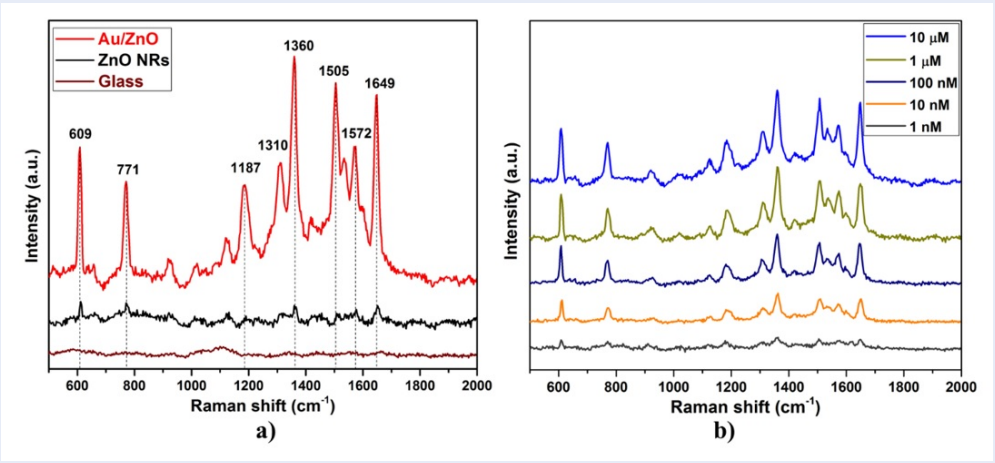

Figure 6: SERS spectra of R6G molecules on the substrates. (a) R6G at 10^{-3} M concentration on glass, ZnO NRs, and Au/ZnO; (b) R6G with different concentrations on Au/ZnO.

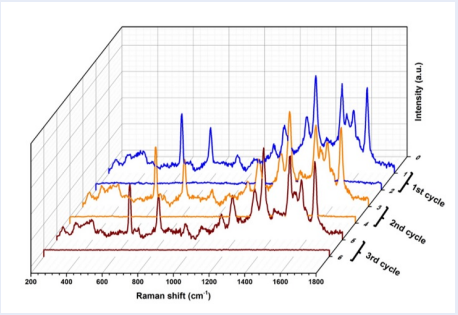

Figure 7: Raman spectra of 10^{-5} M R6G on the Au/ZnO substrate during adsorption/self-cleaning cycles.

by the ZnO NRs, giving rise to the generation of electron-hole pairs on the surface of the ZnO NRs. As a result, the photogenerated electrons can reduce the absorbed Au^{3+} ions to Au^0 by absorbing three electrons for each Au^{3+} ion. At the nucleation site of the initially formed Au nanocrystals on the surface of the ZnO NRs, the subsequent reduction of Au^{3+} ions proceeded at the preexisting nucleation sites and finally resulted in the formation of Au/ZnO heterostructures. Herein, methanol with hydroxyl groups (-OH) served as hole scavengers, giving rise to the inhibition of photogenerated electron-hole recombination by consuming holes. The result will prolong the electron-hole lifetime and thus promote the multielectron reduction of Au^{3+} ions.

The above results demonstrate the successful deposition of Au nanoparticles on ZnO nanorods by the photochemical process, which serves as a 3D hybrid substrate for efficient SERS enhancement. Specifically, the Au composition in the Au/ZnO heterostructure plays a dominant role in the enhanced SERS activity. It is obvious that after attaching Au NPs onto the surface of ZnO NRs, the Raman signal intensity of R6G is significantly enhanced (Figure 6a). The superior SERS performance of the Au/ZnO heterostructure is ascribed to the following factors: *(i)* The photochemical process produces dense Au NPs on the side surfaces and top ends of ZnO nanorods. In addition to localized surface plasmon resonance on Au NPs, the internanoparticle nanogaps formed between the neighboring Au NPs create numerous "hot spots" for strongly enhancing the Raman intensity by an electromagnetic enhancement mechanism (as described in Figure 2d). *(ii)* The 3D Au-NP/ZnO-NR heterostructure with a large surface area facilitates the enhanced number of Au NPs deposited and the increased number of R6G molecules trapped on the surface of the Au/ZnO substrate. The result leads to an effective increase in the hotspot number and interactions of R6G molecules with the Au/ZnO heterostructure and thus strengthens the Raman signal intensity by the electromagnetic enhancement of Au NPs and the chemical enhancement related to charge-transfer interactions between the Au/ZnO substrate and adsorbed R6G molecules under 532 nm laser excitation. All the above explanations lead to the highly sensitive SERS activity of the fabricated Au/ZnO substrate with a low detection limit of 10^{-9} M.

For comparison, these results are consistent with previous reports. Kim *et al.* reported that Au/ZnONRs/G SERS sensors were fabricated by another method using a combination of hydrothermal synthesis and

electron-beam evaporation. These SERS substrates obtained an LOD of 10^{-9} M and an enhancement factor of 2.3x10^6 for R6G[19]. Doan et al. showed that ZnO NRs were fabricated on PCBs by a facile hydrothermal process, and then Au NPs were deposited onto their surface by a sputtering method. The ZnO@Au-based SERS substrate exhibited high sensitivity for detecting other organic molecules, with methylene blue at a low concentration of 10^{-9} M[30]. Chou et al. revealed ZnO NRs decorated with Au NPs using a highly complicated technique via pulsed-laser-induced photolysis. They serve as "hot spots" for the SERS signal of detection of R6G at a low concentration of 10^{-9} M[31]. All of the above studies showed that the high SERS performance of Au nanoparticle/ZnO nanorod substrates is derived from the combination of the localized surface plasmon resonance mode of gold nanoparticles with the charge transfer mode supported by the semiconductor. Therefore, in this study, the Au/ZnO substrate showed superior SERS performance due to the synergistic effects between Au nanoparticles, ZnO nanorods, and adsorbed R6G molecules under 532 nm laser excitation. However, some of the Au NPs synthesized by the photochemical process could be removed from the ZnO NRs after five adsorption/self-cleaning cycles of reuse, so the Au/ZnO substrate is more suitable for rapid analysis techniques.

CONCLUSION

Using the photochemical deposition process, the nanoSERS was made from Au nanoparticles embedded in ZnO nanorods. Furthermore, using methanol as a tunnel solvent increased the lifetime of charge carriers and enhanced the electron reduction of Au^{3+} ions. The findings show that under 532 nm laser stimulation, the Au/ZnO nanostructured substrates have remarkable SERS performance due to the resonance effect of Au nanoparticles, ZnO semiconductors, and R6G organic compounds, and they can detect R6G at concentrations as low as 10^{-9}M. This research adds to the production of highly efficient SERS substrates based on noble metals and semiconductors for the detection of chemicals at low concentrations via surface-enhanced Raman scattering techniques.

LIST OF ABBREVIATIONS

Au NPs: Gold nanoparticles
ZnO NRs: Zinc oxide nanorods
SERS: Surface-enhanced Raman scattering
1D: One-dimensional
2D: Two-dimensional
3D: Three-dimensional
SPR: Surface plasmon resonance
R6G: Rhodamine 6G
LOD: Limit of detection

COMPETING INTERESTS

The authors declare that there is no conflict of interest regarding the publication of this article.

AUTHORS' CONTRIBUTIONS

Nguyen Duy Khanh constructed the present idea and carried out and wrote the manuscript with support from Vu Thi Hanh Thu and Le Vu Tuan Hung.
Luong Minh Thu and Pham Dien Khoa conducted the experiments.
Le Van Ngoc and Le Vu Tuan Hung have supported the analytical techniques.

ACKNOWLEDGMENT

This research is funded by the University of Science, Vietnam National University - Ho Chi Minh, VNU-HCM, under grant number T2018-09.

REFERENCES

1. Chen Y, Liu H, Tian Y, Du Y, Ma Y, Zeng S, Gu C, Jiang T, Zhou J. In situ recyclable surface-enhanced Raman scattering-based detection of multicomponent pesticide residues on fruits and vegetables by the flower-like MoS2@ Ag hybrid substrate. ACS applied materials & interfaces. 2020 Mar 2;12(12):14386-99;PMID: 32118398. Available from: https://doi.org/10.1021/acsami.9b22725.
2. D'Agostino A, Giovannozzi AM, Mandrile L, Sacco A, Rossi AM, Taglietti A. In situ seed-growth synthesis of silver nanoplates on glass for the detection of food contaminants by surface enhanced Raman scattering. Talanta. 2020 Aug 15;216:120936;PMID: 32456888. Available from: https://doi.org/10.1016/j.talanta.2020.120936.
3. Chen M, Liu D, Du X, Lo KH, Wang S, Zhou B, Pan H. 2D materials: Excellent substrates for surface-enhanced Raman scattering (SERS) in chemical sensing and biosensing. TrAC Trends in Analytical Chemistry. 2020 Sep 1;130:115983;Available from: https://doi.org/10.1016/j.trac.2020.115983.
4. Zhang C, Cui X, Yang J, Shao X, Zhang Y, Liu D. Stimulus-responsive surface-enhanced Raman scattering: a "Trojan horse" strategy for precision molecular diagnosis of cancer. Chemical science. 2020;11(24):6111-20;PMID: 34094100. Available from: https://doi.org/10.1039/D0SC01649G.
5. Si Y, Xu L, Wang N, Zheng J, Yang R, Li J. Target microRNA-responsive DNA hydrogel-based surface-enhanced Raman scattering sensor arrays for microRNA-marked cancer screening. Analytical chemistry. 2020 Jan 10;92(3):2649-55;PMID: 31920078. Available from: https://doi.org/10.1021/acs.analchem.9b04606.
6. Qian Y, Meng G, Huang Q, Zhu C, Huang Z, Sun K, Chen B. Flexible membranes of Ag-nanosheet-grafted polyamide-nanofibers as effective 3D SERS substrates. Nanoscale. 2014;6(9):4781-8;PMID: 24658299. Available from: https://doi.org/10.1039/c3nr06483b.
7. Li S, Zhang N, Zhang N, Lin D, Hu X, Yang X. Three-dimensional ordered Ag/ZnO/Si hierarchical nanoflower arrays for spatially uniform and ultrasensitive SERS detection. Sensors and Actuators B: Chemical. 2020 Oct 15;321:128519;Available from: https://doi.org/10.1016/j.snb.2020.128519.

8. Hu W, Xia L, Hu Y, Li G. Recent progress on three-dimensional substrates for surface-enhanced Raman spectroscopic analysis. Microchemical Journal. 2022 Jan 1;172:106908;Available from: https://doi.org/10.1016/j.microc.2021.106908.
9. He RX, Liang R, Peng P, Norman Zhou Y. Effect of the size of silver nanoparticles on SERS signal enhancement. Journal of Nanoparticle Research. 2017 Aug;19(8):1-0;Available from: https://doi.org/10.1007/s11051-017-3953-0.
10. Tsvetkov MY, Khlebtsov BN, Khanadeev VA, Bagratashvili VN, Timashev PS, Samoylovich MI, Khlebtsov NG. SERS substrates formed by gold nanorods deposited on colloidal silica films. Nanoscale research letters. 2013 Dec;8(1):1-9;PMID: 23697339. Available from: https://doi.org/10.1186/1556-276X-8-250.
11. Zhang L, Wang B, Zhu G, Zhou X. Synthesis of silver nanowires as a SERS substrate for the detection of pesticide thiram. Spectrochimica Acta Part A: Molecular and Biomolecular Spectroscopy. 2014 Dec 10;133:411-6;PMID: 24973781. Available from: https://doi.org/10.1016/j.saa.2014.06.054.
12. Sun Y, Zhang Y, Shi Y, Xiao X, Dai H, Hu J, Ni P, Li Z. Facile preparation of silver nanoparticle films as an efficient surface-enhanced Raman scattering substrate. Applied surface science. 2013 Oct 15;283:52-7;Available from: https://doi.org/10.1016/j.apsusc.2013.05.154.
13. Wang Y, Ruan W, Zhang J, Yang B, Xu W, Zhao B, Lombardi JR. Direct observation of surface enhanced Raman scattering in ZnO nanocrystals. Journal of Raman Spectroscopy: An International Journal for Original Work in all Aspects of Raman Spectroscopy, Including Higher Order Processes, and Brillouin and Rayleigh Scattering. 2009 Aug;40(8):1072-7;Available from: https://doi.org/10.1002/jrs.2241.
14. Yang L, Jiang X, Ruan W, Zhao B, Xu W, Lombardi JR. Observation of enhanced Raman scattering for molecules adsorbed on TiO2 nanoparticles: charge-transfer contribution. The Journal of Physical Chemistry C. 2008 Dec 18;112(50):20095-8;Available from: https://doi.org/10.1021/jp8074145.
15. Jiang L, Yin P, You T, Wang H, Lang X, Guo L, Yang S. Highly reproducible surface-enhanced Raman spectra on semiconductor SnO2 octahedral nanoparticles. ChemPhysChem. 2012 Dec 7;13(17):3932-6;PMID: 22997142. Available from: https://doi.org/10.1002/cphc.201200586.
16. Jue M, Lee S, Paulson B, Namgoong JM, Yu HY, Kim G, Jeon S, Shin DM, Choo MS, Joo J, Moon Y. Optimization of ZnO nanorod-based surface enhanced Raman scattering substrates for bioapplications. Nanomaterials. 2019 Mar 17;9(3):447;PMID: 30884889. Available from: https://doi.org/10.3390/nano9030447.
17. Yang B, Jin S, Guo S, Park Y, Chen L, Zhao B, Jung YM. Recent development of SERS technology: Semiconductor-based study. Acs Omega. 2019 Nov 15;4(23):20101-8;PMID: 31815210. Available from: https://doi.org/10.1021/acsomega.9b03154.
18. Pimentel A, Araújo A, Coelho BJ, Nunes D, Oliveira MJ, Mendes MJ, Águas H, Martins R, Fortunato E. 3D ZnO/Ag surface-enhanced Raman scattering on disposable and flexible cardboard platforms. Materials. 2017 Nov 24;10(12):1351;Available from: https://doi.org/10.3390/ma10121351.
19. Kim W, Lee SH, Kim SH, Lee JC, Moon SW, Yu JS, Choi S. Highly reproducible Au-decorated ZnO nanorod array on a graphite sensor for classification of human aqueous humors. ACS applied materials & interfaces. 2017 Feb 22;9(7):5891-9;PMID: 28156092. Available from: https://doi.org/10.1021/acsami.6b16130.
20. Yi Z, Yi Y, Luo J, Li X, Xu X, Jiang X, Yi Y, Tang Y. Arrays of ZnO nanorods decorated with Au nanoparticles as surface-enhanced Raman scattering substrates for rapid detection of trace melamine. Physica B: Condensed Matter. 2014 Oct 15;451:58-62;Available from: https://doi.org/10.1016/j.physb.2014.06.026.
21. Liu C, Xu X, Wang C, Qiu G, Ye W, Li Y, Wang D. ZnO/Ag nanorods as a prominent SERS substrate contributed by synergistic charge transfer effect for simultaneous detection of oral antidiabetic drugs pioglitazone and phenformin. Sensors and Actuators B: Chemical. 2020 Mar 15;307:127634;Available from: https://doi.org/10.1016/j.snb.2019.127634.
22. Sinha G, Depero LE, Alessandri I. Recyclable SERS substrates based on Au-coated ZnO nanorods. ACS applied materials & interfaces. 2011 Jul 27;3(7):2557-63;PMID: 21634790. Available from: https://doi.org/10.1021/am200396n.
23. Solís DM, Taboada JM, Obelleiro F, Liz-Marzán LM, García de Abajo FJ. Optimization of nanoparticle-based SERS substrates through large-scale realistic simulations. ACS photonics. 2017 Feb 15;4(2):329-37;PMID: 28239616. Available from: https://doi.org/10.1021/acsphotonics.6b00786.
24. Liu Y, Zhong M, Shan G, Li Y, Huang B, Yang G. Biocompatible ZnO/Au nanocomposites for ultrasensitive DNA detection using resonance Raman scattering. The Journal of Physical Chemistry B. 2008 May 22;112(20):6484-9;PMID: 18444675. Available from: https://doi.org/10.1021/jp710399d.
25. Wang X, Kong X, Yu Y, Zhang H. Synthesis and characterization of water-soluble and bifunctional ZnO−Au nanocomposites. The Journal of Physical Chemistry C. 2007 Mar 15;111(10):3836-41;Available from: https://doi.org/10.1021/jp064118z.
26. Zhang YX, Zheng J, Gao G, Kong YF, Zhi X, Wang K, Zhang XQ. Biosynthesis of gold nanoparticles using chloroplasts. International journal of nanomedicine. 2011;6:2899;PMID: 22162651. Available from: https://doi.org/10.2147/IJN.S24785.
27. He XN, Gao Y, Mahjouri-Samani M, Black PN, Allen J, Mitchell M, Xiong W, Zhou YS, Jiang L, Lu YF. Surface-enhanced Raman spectroscopy using gold-coated horizontally aligned carbon nanotubes. Nanotechnology. 2012 Apr 30;23(20):205702;PMID: 22543450. Available from: https://doi.org/10.1088/0957-4484/23/20/205702.
28. Raji R, Gopchandran KG. Plasmonic photocatalytic activity of ZnO:Au nanostructures: Tailoring the plasmon absorption and interfacial charge transfer mechanism. Journal of Hazardous Materials. 2019 Apr 15;368:345-57;PMID: 30685723. Available from: https://doi.org/10.1016/j.jhazmat.2019.01.052.
29. Yao C, Chen W, Li L, Jiang K, Hu Z, Lin J, Xu N, Sun J, Wu J. ZnO: Au nanocomposites with high photocatalytic activity prepared by liquid-phase pulsed laser ablation. Optics & Laser Technology. 2021 Jan 1;133:106533;Available from: https://doi.org/10.1016/j.optlastec.2020.106533.
30. Doan QK, Nguyen MH, Sai CD, Mai HH, Pham NH, Bach TC, Nguyen VT, Nguyen TT, Ho KH, Tran TH. Enhanced optical properties of ZnO nanorods decorated with gold nanoparticles for self cleaning surface enhanced Raman applications. Applied Surface Science. 2020 Mar 1;505:144593;Available from: https://doi.org/10.1016/j.apsusc.2019.144593.
31. Chou CM, Thanh Thi LT, Quynh Nhu NT, Liao SY, Fu YZ, Hung LV, Hsiao VK. Zinc oxide nanorod surface-enhanced Raman scattering substrates without and with gold nanoparticles fabricated through pulsed-laser-induced photolysis. Applied Sciences. 2020 Jul 21;10(14):5015;Available from: https://doi.org/10.3390/app10145015.